Detection of some stable species during the oxidation of methane by coupling a jet-stirred reactor (JSR) to cw-CRDS

Chiheb Bahrini, Olivier Herbinet, Pierre Alexandre Glaude, Coralie Schoemaecker, Christa Fittschen, Frédérique Battin-Leclerc

▶ **To cite this version:**

Chiheb Bahrini, Olivier Herbinet, Pierre Alexandre Glaude, Coralie Schoemaecker, Christa Fittschen, et al.. Detection of some stable species during the oxidation of methane by coupling a jet-stirred reactor (JSR) to cw-CRDS. Chemical Physics Letters, 2012, 534, pp.1-7. 10.1016/j.cplett.2012.03.012 . hal-00726381

HAL Id: hal-00726381
https://hal.science/hal-00726381

Submitted on 30 Aug 2012

HAL is a multi-disciplinary open access archive for the deposit and dissemination of scientific research documents, whether they are published or not. The documents may come from teaching and research institutions in France or abroad, or from public or private research centers.

L'archive ouverte pluridisciplinaire **HAL**, est destinée au dépôt et à la diffusion de documents scientifiques de niveau recherche, publiés ou non, émanant des établissements d'enseignement et de recherche français ou étrangers, des laboratoires publics ou privés.

Detection of some stable species during the oxidation of methane by coupling a jet-stirred reactor (JSR) to cw-CRDS

Chiheb Bahrini[a], Olivier Herbinet[a], Pierre-Alexandre Glaude[a], Coralie Schoemaecker[b], Christa Fittschen[b], Frédérique Battin-Leclerc[a]

[a] KINCOM 'Kinetics of Combustion', CNRS – LRGP ENSIC, 1, rue Grandville, BP 20451, 54001 Nancy, France
[b] PhysicoChimie des Processus de Combustion et de l'Atmosphère PC2A, University Lille 1, Cité Scientifique, Bât. C11, 59655 Villeneuve d'Ascq, France

Abstract

We present the coupling of a jet-stirred reactor to detection by cw-CRDS in the near infrared and first results obtained during the oxidation of methane. The mixture is rapidly expanded from the jet-stirred reactor into a 80 cm-long cw-CRDS cell maintained at a the pressure around 1.33 kPa, thus freezing the reaction and decreasing pressure broadening of the absorption lines. Some stable species (CH_4, H_2O and CH_2O) have been quantified through their well structured spectra around 1506 nm, while H_2O_2 and HO_2 radicals could not be detected.

Highlights

► Coupling of cw-CRDS detection to jet-stirred reactor.
► Quantification of CH_4, CH_2O and H_2O in CH_4 oxidation.
► Absence of HO_2 radical detection in CH_4 oxidation system.

Corresponding author
Christa Fittschen
PC2A, University Lille 1, Cité Scientifique, Bât. C11, 59655 Villeneuve d'Ascq, France
E.mail: christa.fittschen@univ-lille1.fr
Tel : + 33 (0)3 20 33 72 66
Fax : + 33 (0)3 20 43 69 77

1. Introduction

Experimental studies of the oxidation of hydrocarbons in apparatuses such as jet-stirred reactors (JSRs) provide data which are needed for the validation of detailed kinetic models. These detailed kinetic models are useful for the development of more efficient and cleaner combustion systems such as engines [1].

One advantage of the jet-stirred reactor is the relatively easy coupling with various types of analytical techniques. Gas chromatography is the most used technique for the quantification and the identification of the species exiting the reactor [2], [3] and [4]. The quantification is usually performed using detectors such as flame ionization detectors (FIDs) and thermal conductivity

detector (TCD). They are well suited for the quantification of stable molecules such as carbon containing molecules (e.g., hydrocarbons, aldehydes, ketones) and permanent gases (e.g., hydrogen, oxygen, carbon oxides). The identification of reaction products is mostly performed using a gas chromatograph coupled to a mass spectrometer with electron impact ionization at 70 eV. Fourier transform infrared spectroscopy (FTIR) can be used for the quantification of water and formaldehyde in the exhaust gas of a jet-stirred reactor [5].

However, these techniques are not adapted to the detection of all species. This is the case for radicals or unstable molecules such as hydroperoxides and ketohydroperoxides, both important intermediates in the low-temperature oxidation of hydrocarbons [6]. Because of their high reactivity, these species are likely to react during the transfer from the reactor to the analytical apparatus. Thus new types of analytical devices were coupled to jet-stirred reactors to try to palliate these problems.

The general idea is to extract samples from the reactor through rapid expansion and to analyze these samples online in order to minimize the time between the sampling and the analysis and thus decrease the possibility of reaction. The coupling of a jet-stirred reactor with a synchrotron vacuum ultra violet-photo-ionization mass spectrometer (SVUV-PIMS) allowed the detection of species with hydroperoxides [6], [7] and [8]. The coupling was achieved through a cone with a very small hole at its top, which was inserted in the wall of the jet-stirred reactor. This cone system allowed maintaining the low pressure in the mass spectrometer and provided a molecular jet for minimization of species collisions. However, this technique was not sensitive enough to detect radical species in the gas phase.

In the present work we coupled a jet-stirred reactor to a new spectroscopic technique: continuous wave cavity ring-down spectroscopy (cw-CRDS) in the near infrared region. The final goal of this coupling is the detection of HO_2 radicals, this technique having proved already its capability to quantify the concentrations of HO_2 radicals [9], [10], [11], [12], [13] and [14]. This Letter presents this new experimental setup as well as first results obtained in the oxidation of methane.

2. Experimental set-up and conditions

The study was performed using a spherical quartz jet-stirred reactor (volume 85 cm^3). Species exiting the reactor were analyzed using two different techniques: gas chromatography and cw-CRDS. While the new coupling between the cell and the reactor is described below, the more classical details about the reactor, the used gas chromatographs, the cw-CRDS set-up, and the cw-CRDS method, are given as Supplementary material.

The cw-CRDS cell (volume 40 cm^3) consists of a glass tube with an outer diameter of 8 mm and a length of 80 cm. The cell is maintained through convection at ambient temperature and at a pressure around 1.33 kPa (10 Torr). The cell is connected to the reactor by the means of a sampling probe, as shown in Figure 1. The probe is a fused silica tube with a diameter of 6 mm and a length of about 10 cm. The extremity of the tube, which is located within the jet-stirred reactor, was thinned by a glass blower such as to have a very small orifice in order to maintain the low pressure in the cw-CRDS cell (the pressure in the reactor is about 106.6 kPa (800 Torr)). This rapid pressure drop freezes the reaction due to a sharp decrease in concentration and temperature, but also leads to a more selective detection due to reduced pressure broadening of the absorption lines. The flow through this orifice into the CRDS cell is estimated to be 90 ccm min^{-1} STP, obtained from measuring the pressure increase in the cw-CRDS cell after closing the pump valve. This flow leads to a residence time of the gas mixture within the CRDS cell of roughly 0.3 s. The same type of sampling probe has already been used to take samples in flames [15].

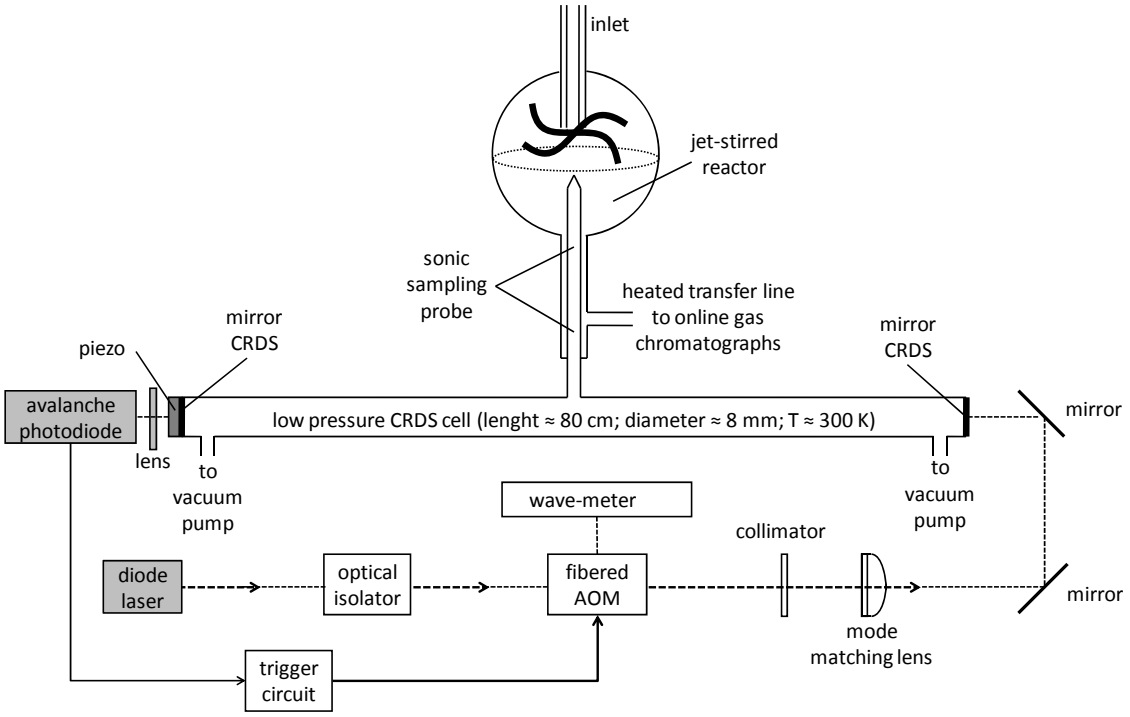

Figure 1. Schematic view of the experimental set-up.

The oxidation of methane was studied at temperatures ranging from 500 to 1300 K, at a residence time of 1 s, and at a reactor pressure of 106.6 kPa. The inlet mole fractions of methane, oxygen and helium were 6.3%, 6.3% and 87.4%, respectively (equimolar mixture of methane and oxygen).

CRDS analysis were carried out in the near infrared at frequencies from 6638 to 6643 cm^{-1} for pressures in the cell between 0.9 and 1.7 kPa. For the species quantified in this work (CH_4, CH_2O and H_2O), we were able to identify absorption lines well isolated from absorption lines of other species. For each experimental condition (residence time, temperature or concentration of gas mixture) we measured a spectrum in the wavelength range 6638–6642.5 cm^{-1} as shown in Figure 2. To obtain this kind of spectrum, we typically average over 50 ring-down signals before incrementing the wavelength of the diode by some 0.0013 cm^{-1}. Due to the rather low resolution of the wavemeter, the wavenumber is registered only for every tenth increment. At the end of the full scan, all data pairs current–wavenumber were fitted through a polynomial and the final wavenumber for each datapoint is then obtained from this polynomial.

Different spectra are shown together in Figure 2: the upper curves are spectra that have been measured in this work, and they are displayed as ring-down time (left y-axis). The lower data (red line and green bars) are spectra taken from the literature: the red line is the CH_2O spectrum from Staak et al. [16] (absorption cross sections in 10^{-21} cm^2, right y-axis), the green bars represents the methane spectrum from Campargue et al. [17] (line strengths in 10^{-24} cm, right y-axis). The shaded areas highlight the sections that have routinely been used for quantifying the three species CH_4 (green), H_2O (blue) and CH_2O (red). The gray shaded area indicates the section that has been represented in Figure 3 as an example for a full model fit: ring-down times have been converted to absorption cross sections α using Eq. (1) (See Supplementary material for details)

$$\alpha = [A] \times \sigma = \frac{R_L}{c}\left(\frac{1}{\tau} - \frac{1}{\tau_0}\right) \quad (1)$$

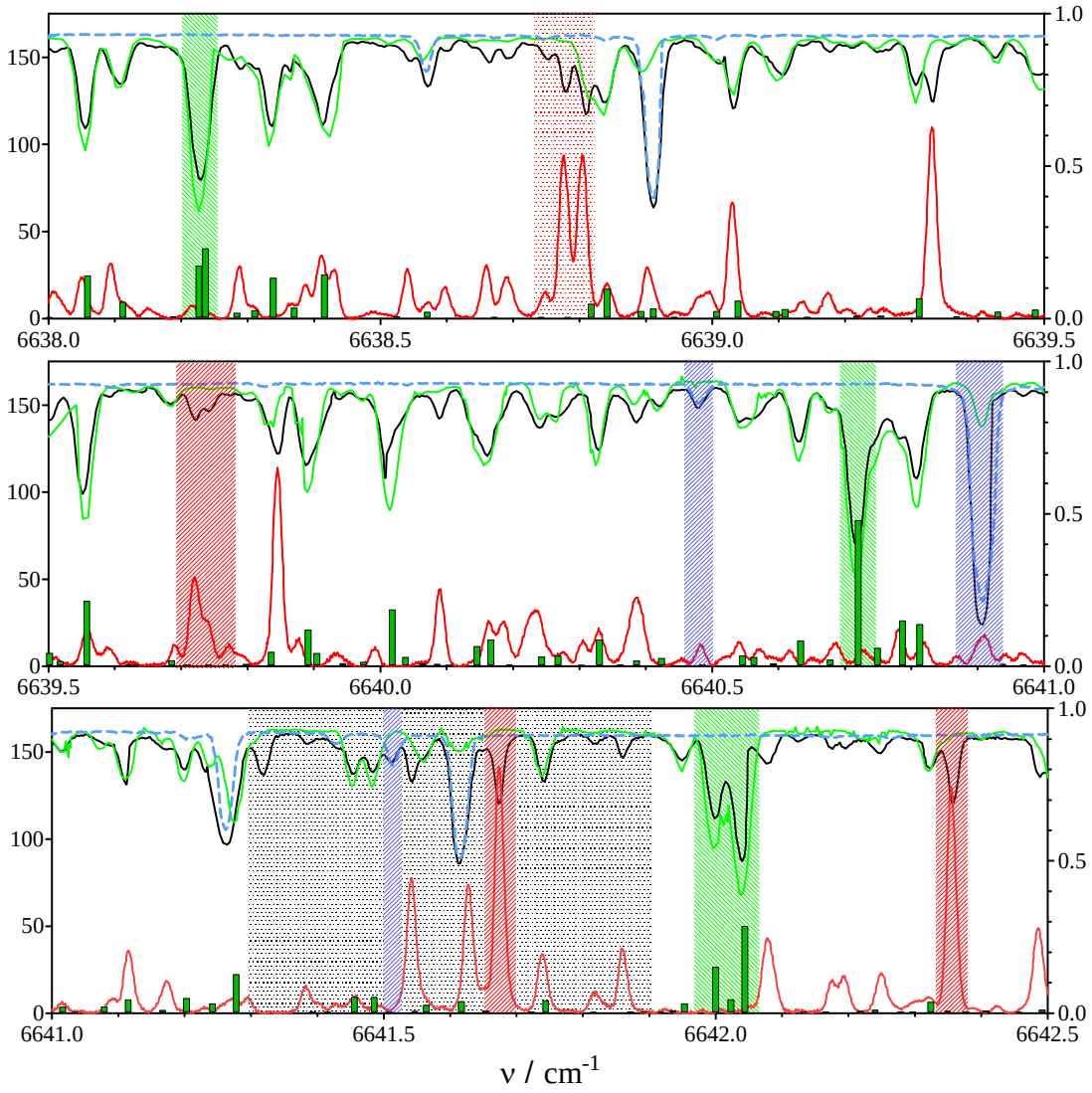

Figure 2. Spectrum from 6638 to 6642.5 cm^{-1}. Left y-axis is ring-down time (μs) for different experiments: (a) green line – 6.3% CH_4, heating off (b) black line – 6.3% CH_4 at Treact = 1113 K and 1 s residence time (c) blue dotted line is H_2O spectrum measured by bubbling small flow through H_2O, right y-axis (d) red line: CH_2O absorption cross-section from Staak et al. [16] (10^{-21} cm^2) (e) green bars: CH_4 line strengths from Campargue et al. [17] (10^{-24} cm). (For interpretation of the references to color in this figure legend, the reader is referred to the web version of this article.)

The Fityk software [18] has been applied to represent the obtained spectrum by the sum of the individual contributions of several species. The spectrum is in agreement by taking only three absorbing species into account: CH_4, CH_2O and H_2O. The ring-down time of the empty cell, i.e. before admitting CH_4 to the main flow, is governed by the reflectivity of the mirrors, and was around 163 μs in the example of Figure 2. The noise of the baseline was around 0.5 μs, indicating a minimum measurable absorption of 7×10^{-10} cm^{-1} (S/N = 1).

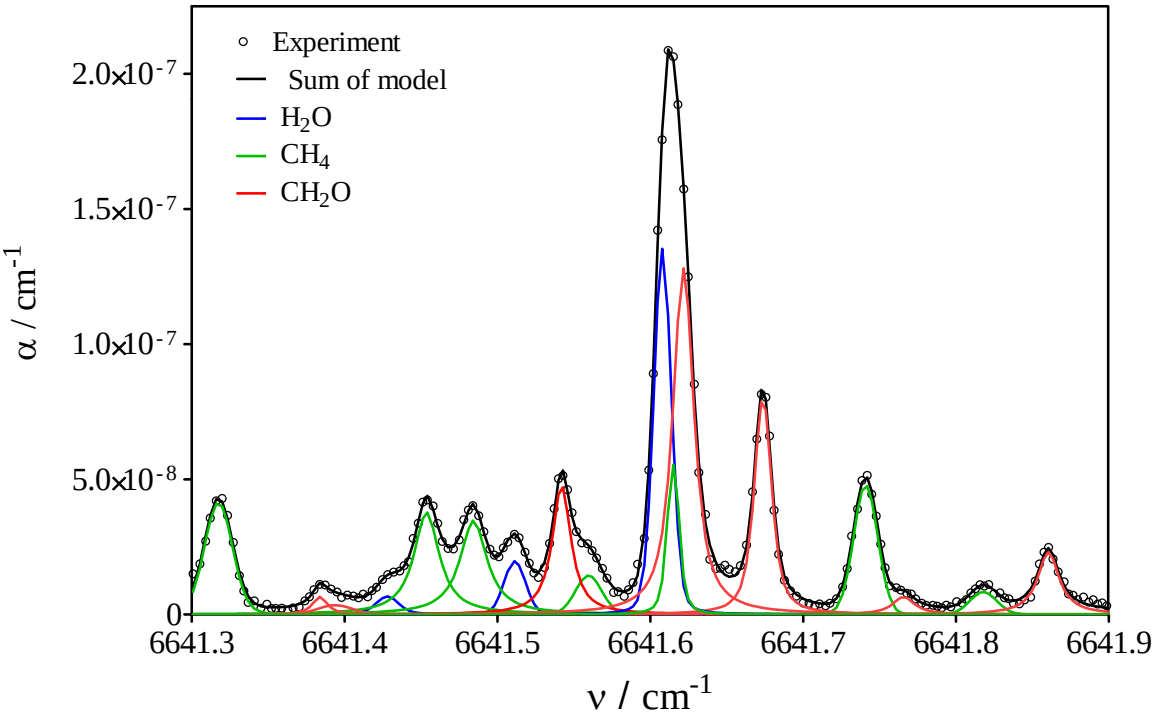

Figure 3. Spectrum from 6641.3 to 6641.9 cm^{-1} (shaded area in Figure 2): open dots are experimental data from Figure 2, full black line is the sum of all individual lines as obtained in Fityk [18].

3. Quantification of CH_4 (reactant) using cw-CRDS

The full green line in Figure 2 shows the spectrum of methane under unreactive conditions (reactor maintained at ambient temperature). A highly congested structure is found, were the line positions and relative intensities are in very good agreement with a recent work of Campargue et al. [17]: the line strengths obtained by these authors are indicated for each individual absorption line as green bars in Figure 2 (right y-axis for line strength units). CH_4 is a stable molecule, and it is admitted into the reactor using calibrated flow meters. Measuring its concentration at room temperature can therefore be used to validate the cw-CRDS set-up. This is especially useful as the absorption path length is not exactly known: a flow of pure He is admitted in front of the mirrors in order to protect them: this flow dilutes the reaction mixture within the cw-CRDS cell, and hence reduces the absorption path length. For deducing a correction factor RL for the path length, we have deduced the absorption cross section σ for the three lines at 6640.72, 6642.00 and 6642.04 cm^{-1} using in Eq. (1) RL = 1 and $[CH_4] = 1.87 \times 10^{16}$ cm^{-3}, obtained from ideal gas law, and have compared it to literature values [17]. We obtain absorption cross sections of 1.81, 0.609 and 1.17×10^{-24} cm^2 for the three above mentioned lines. Taking into account the broadening of the absorption lines, the line strengths from Campargue et al. [17] can be converted to absorption cross sections: for the lines at 6640.72, 6642.00 and 6642.04 cm^{-1}, Campargue et al. have given line strength of S = 4.75, 1.51 and 2.852×10^{-25} cm, respectively: using an average broadening coefficient of 0.05 cm^{-1} atm^{-1} [19], application of a Voigt profile leads to peak absorption cross sections of σ = 2.05, 0.65 and 1.22×10^{-23} cm^2 at 1.13 kPa (8.5 Torr) Helium, i.e. a factor of 1.13, 1.10 and 1.04 larger than our values. Taking the average of this value, we can deduce that the 'real' absorption path is only 73.6 cm (80 cm × 0.92); this value will be used in the following quantification.

The black line in Figure 2 shows the spectrum after turning on the heating and it can be seen that the CH_4 absorption features decrease: according to Eq. (1) an increase in ring-down time τ corresponds to a decrease in absorption. We have extracted the CH_4 concentration using four lines: the above

mentioned three as well as the line at 6638.23 cm^{-1}: this line is a convolution of two individual lines and its absorption cross sections under our conditions can therefore not be compared to the absorption cross section of the individual lines as published by Campargue et al. [17] and hence was not suitable for obtaining the pathlength. The absorption cross section for this line is $\sigma = 1.38 \times 10^{-23}$ cm^2 under our conditions. The example in Figure 2 leads to $[CH_4]$ = 1.11, 1.04 and 1.08 × 10^{16} cm^{-3}, with an average of 1.08 × 10^{16} cm^{-3}, corresponding to a mole fraction of 0.0362. The average of all four lines is used for comparisons.

The results for different temperatures are shown, together with GC data and model calculations, in Figure 4.

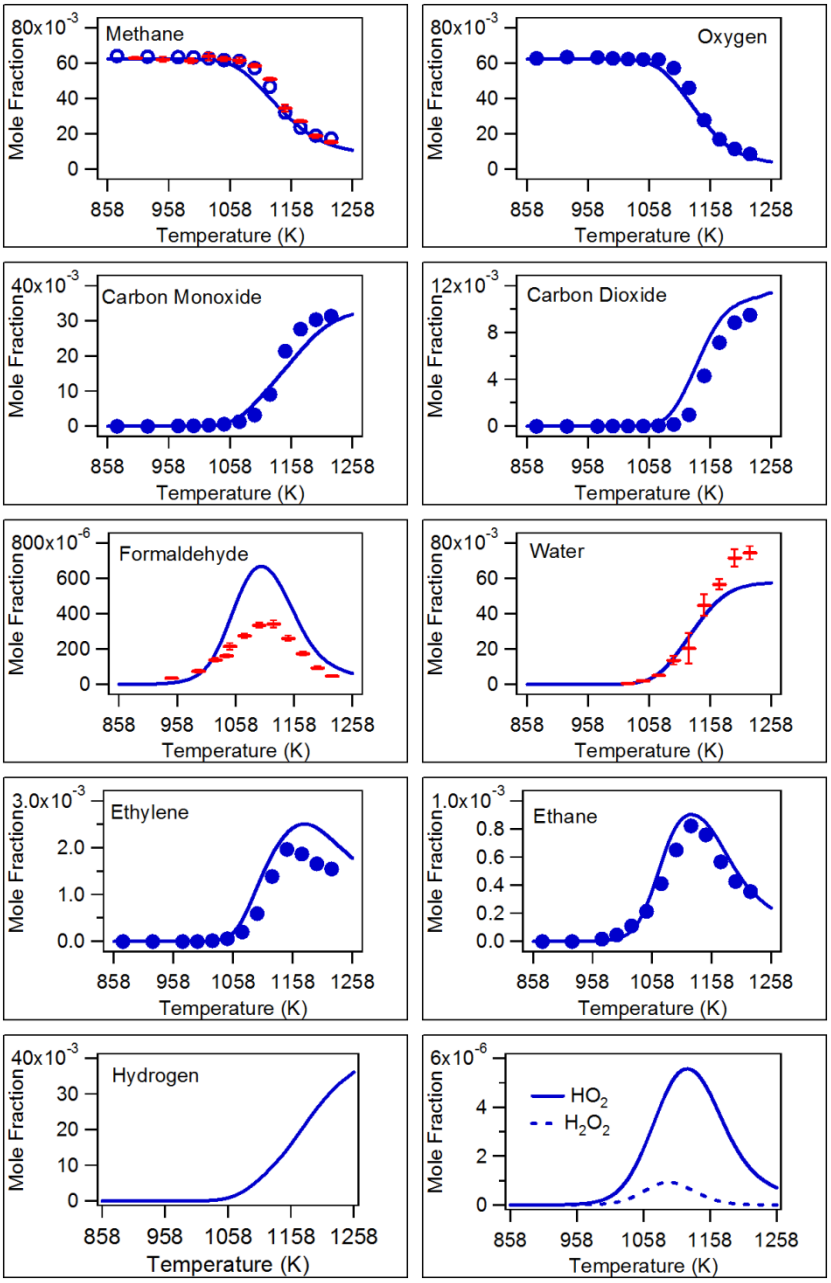

Figure 4. Mole fraction profiles of reactants and reaction products obtained in the study of the oxidation of methane in a jet-stirred reactor (red crosses: cw-CRDS experimental data; blue dots: gas chromatography experimental data in JSR; — computed data). (For interpretation of the references to color in this figure legend, the reader is referred to the web version of this article.)

4. Quantification of formaldehyde CH_2O using cw-CRDS

In order to investigate the formation of products (such as formaldehyde) obtained during the methane oxidation in a jet-stirred reactor, we have compared the spectrum obtained during CH_4-oxidation with the CH_2O spectrum as reported by Staak et al. [16]: the spectrum is shown as a red line in Figure 2 (absolute absorption cross sections in 10^{-21} cm^2 on the right y-axis): areas interesting for CH_2O quantification are shaded in red. The lines at 6638.777, 6638.804, 6641.674 cm^{-1} (see complete fit in Figure 3 for this line) and 6642.355 cm^{-1} are the most intense absorption features in this wavelength range with an absorption cross sections of 5.1, 5.2, 7.8, and 7.2 × 10^{-22} cm^2, respectively. The broad, unresolved absorption feature at 6639.72 cm^{-1} is less intense (2.9 × 10^{-22} cm^2), but is well isolated from absorption lines of other products and could therefore be used for CH_2O quantification. The build-up of formaldehyde molecules in the reactor after turning on the heater can be observed very clearly and without fail. We have calculated the concentration of CH_2O from all four lines in the example of Figure 2 to be 6.81, 6.16, 6.56 and 6.56 × 10^{13} cm^{-3} using the above mentioned absorption cross sections. The average value is used for comparison with the model [7] in Figure 4, and corresponds to a molar fraction of 218 ppm in the example of Figure 2.

5. Quantification of water using cw-CRDS

The absorption spectrum of H_2O has been measured in our set-up by bubbling a small portion of the total flow through liquid water, the obtained spectrum is shown as dashed blue line in Figure 2. The strongest water line at 6640.91 cm^{-1} can also be seen in the CH_4 spectrum at room temperature (green line) due to the residual water in the main Helium flow. This strong absorption line (line strength 3.80 × 10^{-24} cm [20], σ = 1.60 × 10^{-22} cm^2 using broadening coefficient of 0.1 cm^{-1} atm^{-1} [21]) can be used very well for quantification of low H_2O-concentrations, i.e. at lower temperature, however at higher temperature the transition rapidly saturates. Therefore, two smaller lines at 6640.48 and 6641.51 cm^{-1} (shaded in blue in Figure 2) have been used at higher temperatures. In routine analysis we have extracted the concentration by applying Eq. (1) and taking as baseline τ_0 the average of the baseline just left and right off the peak absorption. This simple approximation is a very good agreement with the complete fit using the Fityk software [18]. In Figure 3 we have presented such a complete fit for a small portion of the spectrum (gray area in Figure 2): from this fit, we obtain for the small H_2O-line at 6641.51 cm^{-1} an area of 2.86 × 10^{-10} cm^{-2}, which converts to $[H_2O]$ = 3.2 × 10^{15} cm^{-3} by using the line strength of 8.82 × 10^{-26} cm from Macko et al. [20]. Using the simple method, we calculate α = 1.17 × 10^{-8} cm^{-1} (τ_0 = (152.4 + 148.5)/2 µs and τ = 143.5 µs). Using a broadening coefficient [21] of 0.1 cm^{-1} atm^{-1}, we obtain σ = 3.71 × 10^{-24} cm^2 using a Voigt profile: this value leads to a concentration of $[H_2O]$ = 3.16 × 10^{15} cm^{-3}, in excellent agreement with the full model.

6. Reactants and reaction products mole fraction profiles

The evolution of the mole fractions of the reactants and of the reaction products were recorded as a function of the temperature (Figure 4). Ten species were detected in this study: carbon oxides, ethylene, ethane, propene, propane, formaldehyde and water. Carbon oxides, ethylene, ethane, propene, propane as well as methane and oxygen were quantified using gas chromatography (propane and propene data are not displayed in Figure 4 because these species were detected in very low concentrations). cw-CRDS was used to quantify methane, water and formaldehyde; the last two being not quantifiable by GC–FID.

As shown in Figure 4, there is a very good agreement for methane between both types of detection, cw-CRDS and gas chromatography, over the whole temperature range. Methane is a rather stable hydrocarbon and starts to react at around 1058 K. Formaldehyde, ethylene and ethane have the typical mole fraction profiles of intermediate species with a maximum (e.g., maximum at 1098 K for

formaldehyde). Carbon oxides and water have mole fractions increasing on the whole investigated temperature range.

Carbon and oxygen atom balances were performed between the inlet and the outlet of the reactor using experimental mole fractions of species (the number of atoms which disappeared in the reactants was compared to the number of atoms in the quantified reaction products). Carbon and oxygen atom balances were satisfactory (the difference is lower than 10%).

A detailed kinetic model for the oxidation of methane [7] and [22] was used to perform simulations. Computed data are also displayed in Figure 4. The model reproduces well the consumption of the reactants. The agreement is overall satisfactorily for reaction products, except for formaldehyde. For this species, computed mole fractions are about twice as large as the experimental ones. A kinetic analysis of the model performed at 1100 K showed that formaldehyde is mainly formed from the methyl radical by two pathways. The most important one is the sequence of reactions CH3 + HO2 = CH_3O + OH and CH_3O = H + CH_2O (61% of the formation of formaldehyde). The second one is the reaction CH_3 + O_2 = CH_2O + OH (22% of the formation of formaldehyde). Note that the kinetic parameters used in the model for the reaction CH_3 + HO_2 = CH_3O + OH are significantly uncertain. They come from the review by Baulch et al. [23] in which a large uncertainty factor of five is given. The over-prediction of the mole fraction of formaldehyde by the model can be due to this uncertainty. However, to bring the concentration of formaldehyde closer to the experimental one needs to divide the rate constant by at least a factor of five. In this case the global agreement of the simulation gets much worse: the reactivity decreases and simulation profiles are shifted towards higher temperatures.

7. Absence of detection of HO_2 and H_2O_2

CRDS is a technique too sophisticated to be only used for the analysis of species such as formaldehyde and water: these two species can easily be analyzed using Fourier Transform Infrared spectroscopy. The main goal of coupling the cw-CRDS technique to the JSR is the detection of species such as H_2O_2 and HO_2, which also have a well-structured and well-known IR spectrum in the region 1.49–1.51 µm [13] and [17] and are difficult to detect by other techniques.

H_2O_2 has already been detected by cw-CRDS [9] and [13] and presents a well-structured absorption spectrum with some absorption lines calibrated in the emission range accessible to the diode used in this work. The absorption cross section for the absorption line at 6639.88 cm^{-1} of H_2O_2 has already been measured [9], however this line is superposed by an absorption line of CH_4, as can be seen in Figure 5. Next to this line, a smaller line can be found at 6639.77 cm^{-1}, completely unperturbed by any CH_4 line. From a comparison with the calibrated line, we estimate the absorption cross section to be around 5×10^{-23} cm^2, and under the condition of Figure 5, the minimum detectable concentration of H_2O_2 in the presence of large amounts of CH_4 can be estimated to about 4×10^{13} cm^{-3}, corresponding to about 130 ppm. In the present study it has not been possible to detect H_2O_2 because its expected concentration (below 1 ppm according to simulation as shown in Figure 4) is well below the detection limit.

An attempt to detect HO_2 radical has also been made, but without success as shown in Figure 6: the red line shows the spectrum, obtained from the oxidation of 6.3% CH_4 at 1113 K, while the black line shows the spectrum of HO2 radicals such as obtained by Thiebaud et al. [24]. The absorption line at 6638.73 cm^{-1} is with $\sigma = 9.4 \times 10^{-20}$ cm^2 at 50 Torr He ($\approx 1.3 \times 10^{-19}$ cm^2 at 10 Torr using a broadening coefficient of 0.057 cm^{-1} atm^{-1} [25]) not the strongest line in this wavelength range, but it has the advantage that it is not perturbed by other absorbing species. The detection limit under these conditions is around 7×10^9 cm^{-3}, corresponding to 0.02 ppm, well below the concentration of 6 ppm (see Figure 4) predicted by the model.

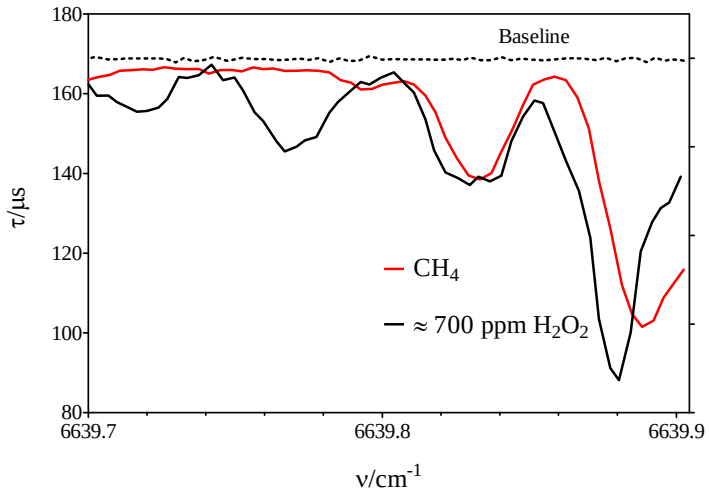

Figure 5. Red line: zoom of the absorption spectrum obtained for 6.3% CH_4 at 1113 K, 1 s residence time. Black dotted line: baseline before admitting CH_4 to the reactor. Full black line: spectrum of H_2O_2, obtained by bubbling a part of the flow through 50% H_2O_2 solution before flowing through the reactor at room temperature. The H_2O_2 concentration is estimated to be around 700 ppm, therefore an upper limit of 130 pmm is estimated from the absence of any absorption around 6639.77 cm^{-1}. (For interpretation of the references to color in this figure legend, the reader is referred to the web version of this article.)

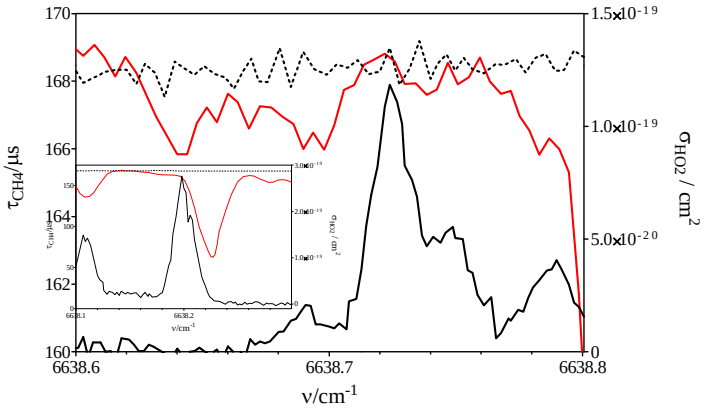

Figure 6. Red line: zoom of the absorption spectrum obtained for 6.3% CH_4 at 1113 K, 1 s residence time. Black dotted line: baseline before admitting CH_4 to the reactor. Full black line: HO_2 absorption spectrum, obtained by Thiebaud et al. [24]. Absence of any absorption at the rather small line at 6638.72 cm^{-1} ($\sigma_{(6.66\ kPa)} \approx 1.3 \times 10^{-19}$ cm^2 at 1.33 kPa) leads to an upper limit of 0.02 ppm HO_2 in the cw-CRDS cell. Note, that the strongest line in this wavelength region at 6638.20 cm^{-1} ($\sigma_{(6.66\ kPa)} = 2.79 \times 10^{-19}$ cm^2) is slightly perturbed by a CH_4 line, as shown in the inset. However, this line might lead to an even lower detection limit for HO_2 for other species. (For interpretation of the references to color in this figure legend, the reader is referred to the web version of this article.)

A possible reason for this absence is that HO_2 radicals are lost during sampling. Radical species are very reactive and their lifetime is very sensitive to their environment. Their reactivity in the gas phase due to self-recombination can be neglected at the expected low concentrations after expansion into the cw-CRDS cell: at 10^{10} molecules cm^{-3} and a self-recombination rate constant of $k = 1.7 \times 10^{-12}$ cm^3 s^{-1} [26], a decay of only 3% of the initial HO_2 concentration can be calculated for a residence time of 1 s in the cw-CRDS cell. However, collisions with the wall of the reactor or the cw-CRDS cell can lead to

heterogeneous recombination reactions and thus to radical loss. In a recent work it has been found, that HO_2 radicals disappeared very efficiently on the walls of a large photoreactor made of quartz [27]. In another recent work, the very efficient loss of HO_2 radicals due to heterogeneous recombination on glass surfaces has even been exploited as a selective detection of HO_2 and RO_2 radicals [28].

8. Conclusion

The coupling of a jet-stirred reactor to a set-up for cw-CRDS detection was performed for the first time. The experimental study of the oxidation of methane was carried out using two analytical techniques simultaneously, the classical gas chromatography and the new cw-CRDS. The very good agreement between the two sets of data obtained for the concentration of methane with both analytical techniques allowed the validation of the cw-CRDS as a detection method for probing the outlet of a jet-stirred reactor. The cw-CRDS technique was used also for the quantification of H_2O and CH_2O.

An unsuccessful attempt of detection and quantification of H_2O_2 and HO_2 radicals was also performed. While the predicted mole fraction of H_2O_2 is below the detection limit of cw-CRDS (130 ppm), detailed kinetic models predicted mole fractions well above the detection limits in the case of HO_2 radicals (0.02 ppm). The absence of HO_2 radicals is probably due to the heterogeneous loss of these very unstable species on the wall inside the JSR and/or of the probe during the sampling. Future investigations will be carried out in order to detect both species, including studies of more reactive species, such as butane in order to obtain higher H_2O_2 mole fractions at lower temperatures, and of ways for minimizing wall effects.

Acknowledgments

This work was supported by the European Commission ('Clean ICE' ERC Advanced Research Grant) and the COST Action CM0901 (EU). The authors thank Ophélie Frottier for the help in gas chromatographic analyses.

Appendix A. Supplementary data

Detailed description of the experimental set up

References

[1] F. Battin-Leclerc et al., Chem. Soc. Rev. 40 (2011) 4762.
[2] P.A. Glaude, O. Herbinet, S. Bax, J. Biet, V. Warth, F. Battin-Leclerc, Combust. Flame 157 (2010) 2035.
[3] W.K. Metcalfe, C. Togbé, P. Dagaut, H.J. Curran, J.M. Simmie, Combust. Flame 156 (2009) 250.
[4] S. Jahangirian, S. Dooley, F.M. Haas, F.L. Dryer, Combust. Flame 159 (2012) 30.
[5] B. Rotavera, P. Diévart, C. Togbé, P. Dagaut, E.L. Petersen, Proc. Combust. Inst. 33 (2011) 175.
[6] F. Battin-Leclerc et al., Angew. Chem. Int. Ed. 49 (2010) 3169.
[7] O. Herbinet et al., Phys. Chem. Chem. Phys. 13 (2011) 296.
[8] F. Battin-Leclerc et al., Proc. Combust. Inst. 33 (2011) 325.
[9] C. Bahrini, A. Parker, C. Schoemaecker, C. Fittschen, Appl. Catal. B-Environ. 99 (2010) 413.
[10] Z.-W. Liu, Y. Xu, X.-F. Yang, A.-M. Zhu, G.-L. Zhao, W.-G. Wang, J. Phys. D: Appl. Phys. 41 (2008).
[11] C. Jain, C. Schoemaecker, C. Fittschen, Z. Phys. Chem. 225 (2011) 1105.
[12] J. Thiébaud, C. Fittschen, Appl. Phys. B Lasers O 85 (2006) 383.
[13] A.E. Parker, C. Jain, C. Schoemaecker, P. Szriftgiser, O. Votava, C. Fittschen, Appl. Phys. B 103 (2011) 725.

[14] C. Jain, A.E. Parker, C. Schoemaecker, C. Fittschen, ChemPhysChem 11 (2010) 3867.
[15] E. Pousse, Z.Y. Tian, P.A. Glaude, R. Fournet, F. Battin-Leclerc, Combust. Flame 157 (2010) 1236.
[16] M. Staak, E.W. Gash, D.S. Venables, A.A. Ruth, J. Mol. Spectrosc. 229 (2005) 115.
[17] A. Campargue, L. Wang, A.W. Liu, S.M. Hu, S. Kassi, Chem. Phys. 373 (2010) 203.
[18] M. Wojdyr, J. Appl. Cryst. 43 (2010) 1126.
[19] C. Frankenberg, T. Warneke, A. Butz, I. Aben, F. Hase, P. Spietz, L.R. Brown, Atmos. Chem. Phys. 8 (2008) 5061.
[20] P. Macko et al., J. Mol. Spectrosc. 227 (2004) 90.
[21] G. Durry, V. Zeninari, B. Parvitte, T. Le Barbu, F. Lefevre, J. Ovarlez, R.R. Gamache, J. Quant. Spectrosc. Radiat. 94 (2005) 387.
[22] P. Barbe, F. Battin-Leclerc, G.M. Côme, J. Chim. Phys. 92 (1995) 1666.
[23] D. Baulch et al., J. Phys. Chem. Ref. Data 21 (1992) 411.
[24] J. Thiebaud, S. Crunaire, C. Fittschen, J. Phys. Chem. A 111 (2007) 6959.
[25] R. Atkinson et al., Atmos. Chem. Phys. 4 (2004) 1461.
[26] N. Ibrahim, J. Thiebaud, J. Orphal, C. Fittschen, J. Mol. Spectrosc. 242 (2007) 64.
[27] M. Djehiche, A. Tomas, C. Fittschen, P. Coddeville, Z. Phys. Chem. 225 (2011) 983.
[28] K. Miyazaki, A.E. Parker, C. Fittschen, P.S. Monks, Y. Kajii, Atmos. Meas. Tech. 3 (2010) 1547.